



**HAL**  
open science

## Measurements of He-collision-induced line-shape parameters of CO<sub>2</sub> lines in the $\nu_3$ band

F. Hendaoui, D. Jacquemart, A. Hessani, B. Tremblay, H. Aroui, H. Tran

► **To cite this version:**

F. Hendaoui, D. Jacquemart, A. Hessani, B. Tremblay, H. Aroui, et al.. Measurements of He-collision-induced line-shape parameters of CO<sub>2</sub> lines in the  $\nu_3$  band. *Journal of Quantitative Spectroscopy and Radiative Transfer*, 2025, 334, pp.109361. 10.1016/j.jqsrt.2025.109361 . hal-04955030

**HAL Id: hal-04955030**

<https://hal.sorbonne-universite.fr/hal-04955030v1>

Submitted on 18 Feb 2025

**HAL** is a multi-disciplinary open access archive for the deposit and dissemination of scientific research documents, whether they are published or not. The documents may come from teaching and research institutions in France or abroad, or from public or private research centers.

L'archive ouverte pluridisciplinaire **HAL**, est destinée au dépôt et à la diffusion de documents scientifiques de niveau recherche, publiés ou non, émanant des établissements d'enseignement et de recherche français ou étrangers, des laboratoires publics ou privés.

# Measurements of He-collision-induced line-shape parameters of CO<sub>2</sub> lines in the $\nu_3$ band

F. Hendaoui<sup>1,2</sup>, D. Jacquemart<sup>3</sup>, A. Hessani<sup>3</sup>, B. Tremblay<sup>3</sup>, H. Aroui<sup>2</sup>, H. Tran<sup>1,\*</sup>

<sup>1</sup> *Laboratoire de Météorologie Dynamique, IPSL, Sorbonne Université, ENS, Université PSL, École polytechnique, Institut Polytechnique de Paris, CNRS, Paris, France*

<sup>2</sup> *Université de Tunis, Laboratoire de Spectroscopie et Dynamique Moléculaire, Ecole Nationale Supérieure d'Ingénieurs de Tunis, 5 Av. Taha Hussein, 1008 Tunis, Tunisia*

<sup>3</sup> *Sorbonne Université, CNRS, MONARIS, UMR 8233, 4 place Jussieu, 75005 Paris, France*

## Abstract

He-collision-induced line-shape parameters of CO<sub>2</sub> lines were measured in the  $\nu_3$  band using Fourier transform spectra recorded at room temperature and with pressures ranging from 263 mbar to 1106 mbar. The measured transmission spectra were analyzed with the Voigt profile combined with the first-order line-mixing approximation, accounting for the instrument line-shape function. The He-broadening coefficients, pressure shifts, and first-order line-mixing parameters were determined for 51 lines, from the  $P(50)$  to the  $R(51)$ . The obtained He-broadening coefficients are in excellent agreement with various literature values. These broadening coefficients, together with data for higher  $J$  lines, extrapolated from available high-temperature measurements, allowed us to propose an improved dataset for He-broadening coefficients of CO<sub>2</sub> lines. We demonstrated that accounting for line-mixing effects is essential to accurately determine the pressure shifts. The latter, measured for the first time for the  $\nu_3$  band, exhibited a weak rotational dependence, in contrast to the strong dependence observed for air- and self-pressure shifts for CO<sub>2</sub>. The obtained line-mixing coefficients agree well with those calculated using the Energy Corrected Sudden model. The results of this study significantly enhance the line-shape parameters dataset for CO<sub>2</sub> perturbed by He, providing improved data for spectroscopic databases and for studies of planetary and exoplanetary atmospheres.

## 1. Introduction

Knowledge of He-collision-induced line-shape parameters for CO<sub>2</sub> lines is essential for atmospheric opacity calculations for some gas giants as Jupiter, Saturn and Uranus [1,2]. Accurate and comprehensive line-shape parameters of CO<sub>2</sub> in He, across wide temperature and pressure ranges, are also critical for radiative modeling and characterization of exoplanet atmospheres [3,4]. He-broadening coefficients for CO<sub>2</sub> lines were included in the HITRAN database for the first time in its 2020 edition [5,6], based on values measured at room temperature of Ref. [7]. The temperature dependence of line broadening in HITRAN comes from measurements reported in Refs. [8,9] for lines with rotational quantum number  $J$  up to 20, while a constant value of 0.58 is applied for  $J$  larger than 20 [5]. Although this update covers a limited dataset, it represents a significant advance for spectroscopic databases, so far mainly

---

\* Corresponding author: ha.tran@lmd.jussieu.fr

devoted to earth atmospheric conditions. It highlights the need for precise experimental and theoretical determinations of broadener-specific line-shape parameters.

Several published papers are focused on the calculation and measurement of He-broadened CO<sub>2</sub> line-shape parameters (e.g. [7,9-14]). In Ref. [10], He-broadening and shifting coefficients were measured at room temperature for 24 lines in the 3  $\nu_3$  band of CO<sub>2</sub>, from the *P*(36) to the *R*(13) lines, using a Fourier transform spectrometer. In 2000, the same group measured He-broadening coefficients for several CO<sub>2</sub> lines in the  $\nu_3$  band [12], for temperatures ranging from 123 K to 760 K. Close-coupling calculations were also performed, initially reported in Ref. [12] and then improved in Ref. [13], demonstrating good agreement with measured values. More recently, Ref. [7] utilized a continuous-wave cavity ring-down spectrometer to measure He-broadening coefficients for five CO<sub>2</sub> lines in the 3 $\nu_1$ + $\nu_3$  band in the 263 - 326 K temperature range. They were able to determine the temperature exponent for only one CO<sub>2</sub> line, obtaining a value of 0.3. Note that the measured line broadening coefficients reported by Ref. [7] are significantly smaller than those obtained by Ref. [10]. He-broadening coefficients for the *R*(11) and *P*(2) lines in the  $\nu_3$  band of <sup>13</sup>CO<sub>2</sub> were measured in Ref. [9] for various temperatures, from 70 K to 300 K. The measured data [9] were found to agree well with values computed using quantum scattering calculations together with the potential energy surface developed in Ref. [13]. In Ref. [14], He-broadening coefficients for four  $\nu_3$  CO<sub>2</sub> lines, from *R*(63) to *R*(69), were measured at room temperature using the speed-dependent Voigt profile. Figure 1 illustrates the He-broadening coefficients measured at room temperature in these various studies, as well as the data adopted in HITRAN 2020.

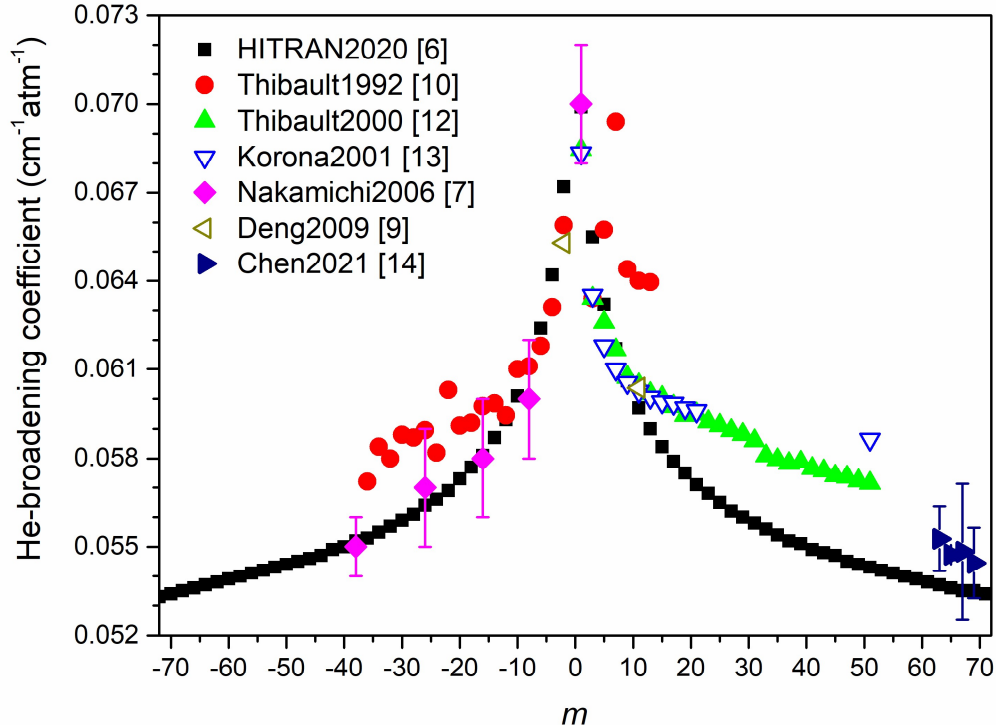


Figure 1: Measured and calculated He-broadening coefficients of CO<sub>2</sub> lines at room temperature from literature, and comparison to values adopted in the HITRAN database [6]. These values are plotted versus  $m$ , with  $m = -J$  and  $m = J + 1$  in the *P* and *R* branches, respectively.

As shown in Fig. 1, significant differences, up to 5%, are observed between various data sources. Extrapolating these data to high  $J$  lines and/or for other temperatures may result in even larger discrepancies. In the present work, the He-collision line-shape parameters of CO<sub>2</sub> lines are revisited using high-resolution laboratory measurements. To this end, a high-resolution Fourier transform spectrometer is used to record spectra of CO<sub>2</sub> highly diluted in He in the 4.3  $\mu\text{m}$  spectral range, at room temperature and pressures ranging from 263 to 1106 mbar. The recorded spectra were then analyzed using the Voigt profile, with the first-order line-mixing accounted for, to retrieve the corresponding line-shape parameters, i.e. the line broadening coefficients, the pressure shifts and the first-order line-mixing coefficients. A detailed uncertainty analysis of the obtained parameters is carried out, considering uncertainties from various sources. Comparisons of the obtained line-shape parameters with data available in literature are conducted from which recommended line-shape parameters for CO<sub>2</sub> lines broadened by He are proposed for database and applications.

This paper is organized as follows: in Sec. 2, we present the experimental setup, measurement procedure and conditions, as well as the determination of the instrument line-shape function. The line-shape model and fitting procedure are detailed in Sec. 3, along with an explanation of the uncertainty budget determination. The obtained line-shape parameters are presented and discussed in Sec. 4, while conclusions and perspectives of this work are provided in Sec.5.

## 2. Experimental setup and procedure

Fourier transform spectra were recorded at the MONARIS laboratory using a Bruker IFS-120 HR spectrometer connected to a White-type cell with base length of 1 m. The total absorption path length was 415 cm, and the Bruker spectral resolution was  $0.01\text{ cm}^{-1}$ , corresponding to a maximum optical path difference of 90 cm. The instrument was equipped with a tungsten source, a 2.0 mm diameter entrance aperture, a collimator with a focal length of 418 mm, a KBr beamsplitter and an InSb detector. No artificial optical weighting was performed (a boxcar function was selected). A Mertz procedure [15] was used to correct the phase of the average interferogram. The measurements were performed as follows: the cell was first filled with a very small quantity of CO<sub>2</sub> (0.0028 mbar, measured with a 1-mbar full-scale Baratron gauge), and then completed with He to reach a total pressure of 263 mbar, followed by 491 mbar, 696 mbar, and 1106 mbar. The carbon dioxide and helium commercial samples from Air Liquide were used without purification (99.9% natural CO<sub>2</sub>; 99.995% He). The total pressures were measured with a 1000-mbar full-scale Baratron gauge, of stated uncertainty of 0.5%. At each desired total pressure, once the sample was well mixed, a spectrum was recorded by adding over 1800 scans during 18 hours. An empty cell spectrum was also recorded under the same optical conditions (after pumping down to a pressure  $< 10^{-4}$  mbar), providing the 100% transmission level and allowing to remove partially the multiplicative channel due to interferences on parallel faces from the windows of the cell and the optical filter. The amplitude (peak-to-peak) of the remaining channel is around 0.3%. For each pressure, the corresponding transmission spectrum was obtained by dividing the signal with gas by the empty cell spectrum. A signal-to-noise ratio of about 700 was obtained for the transmission spectra. The variation of the total pressure during 18 hours is around  $2 \cdot 10^{-4}$  mbar. The average temperature during recordings is about 294 K, with an accuracy of  $\pm 0.1$  K. The experimental pressures and temperatures of the recorded spectra are summarized in Table 1. Note that, due to the very weak quantity of CO<sub>2</sub> gas (a few  $10^{-3}$  mbar), to possible partial gas adsorption by the cell wall and small leaks during gas filling, the partial pressure of CO<sub>2</sub> in the mixture is not known with high

precision. However, since the absolute line intensity is not of interest in this work, and because this quantity is very small, the uncertainty of the CO<sub>2</sub> pressure does not affect the measured He-collision-induced line shape of the considered CO<sub>2</sub> transitions. Also, since the line positions at zero pressure are not of interest in this work, no wavenumber calibration was performed. The four experimental spectra being recorded using identical optical settings, the relative calibration between spectra can be assumed, allowing the retrieval of pressure-shift coefficients.

Two pure CO<sub>2</sub> spectra were also recorded, one with a pressure of 0.0087 mbar (denoted spectrum 0 in Table 1) in order to derive the instrument line shape (ILS) using the LINEFIT14.8 software [16,17] and the other with a pressure of 30 mbar in order to check through saturated CO<sub>2</sub> transitions that the zero of the signals is satisfactory (saturation of  $I/I_0$  observed around  $1.5 \cdot 10^{-4}$ ). Tests were conducted to ensure that the spectral range considered for the obtained ILS was large enough by fitting several pure and He-broadened CO<sub>2</sub> lines and varying the ILS spectral range width. The results showed that a spectral range of  $1.1 \text{ cm}^{-1}$  is sufficient.

Spectrum number	$P_{\text{CO}_2}$ ( $10^{-3}\text{atm}$ )	$P_{\text{tot}}$ (atm)	$T$ (K)
0	$\sim 0.0086$	$\sim 0.0086$	293.9
1	$\sim 0.0027$	0.2600	294.1
2	$\sim 0.0027$	0.4846	294.7
3	$\sim 0.0027$	0.6864	294.6
4	$\sim 0.0027$	1.0911	293.6

Table 1: Experimental pressure and temperature conditions of recorded spectra.

### 3. Spectra analysis

The measured transmission spectra were analyzed using a multi-fitting procedure with our own fitting code. This code can use different line-shape models, from the simple Voigt profile to the Hartmann-Tran profile [18,19]. In the present study, due to the limited signal-to-noise ratio of the measurements, only two profiles could be used in the analysis: the simple Voigt profile (VP) and the Voigt profile with first-order line-mixing (LM). The instrument line-shape function, determined from the pure CO<sub>2</sub> spectrum measured at low pressure as explained in Sec. 2, was then fixed and accounted for in the fits of the He-broadened spectra. For each line, a spectral range of about  $2 \text{ cm}^{-1}$  around the line was considered in the fits. All lines with integrated line intensity greater than  $1.3 \cdot 10^{-19} \text{ cm}^{-1}/(\text{molec.cm}^{-2})$  were fitted. The contribution of weaker lines was calculated based on the measured experimental conditions and using spectroscopic data from the HITRAN database [6]. For this calculation, the partial pressure of CO<sub>2</sub> for each spectrum was redetermined using the fitted areas and integrated intensities in HITRAN for several  $\nu_3$  lines of <sup>12</sup>CO<sub>2</sub>. For each considered spectral range and for each pressure, a linear base line for the 100% transmission was fitted. The line area and maximum absorption position (thus including the zero-pressure line position and the collision-induced pressure shift) were also fitted for each spectrum. The other line-shape parameters, i.e., the broadening coefficient and the first-order line-mixing parameter, were constrained to be the same for the four measured spectra. Figure 2 displays some examples of the measured transmissions and the corresponding fit residuals obtained for different lines. The remaining residuals are mainly due to the multiplicative channels on the measured spectra. Note that considering line-mixing effects in the spectra analysis led to only slightly better residuals compared to the use of a simple Voigt

profile, but to large differences in the retrieved pressure-shift coefficients, as demonstrated in the next section.

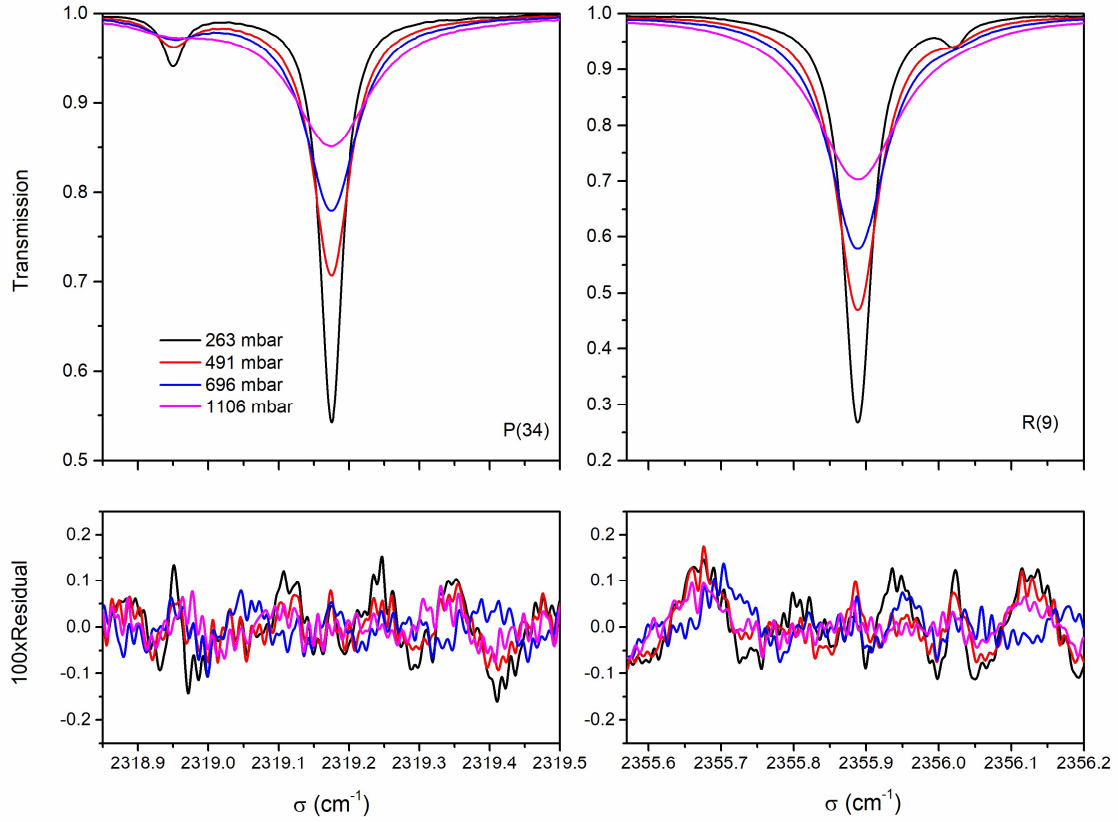


Figure 2: Examples of measured transmissions along with their fit residuals obtained by fitting the measured spectra with the Voigt profile together with the first-order line-mixing approximation.

The uncertainty of the fitted parameters comes from different sources. The first one is the statistical uncertainty (type B), corresponding to the standard deviation obtained from the fits. This quantity is negligibly small compared to the systematic uncertainties. The latter arise from uncertainty in the measured pressure, temperature, and the apparatus function. In our analysis, we assumed that the total pressure,  $P_{tot}$ , is directly equal to the partial pressure of He. This assumption has a largely negligible effect on the determined He collision-induced line-shape parameters since the concentration of  $\text{CO}_2$  in the mixtures should be smaller than 0.00106% ( $P_{\text{CO}_2}$  is about 0.0028 mbar while  $P_{tot}$  is at least 263 mbar). To determine the uncertainty due to errors in the measured  $P_{tot}$ , we reanalyzed the four measured spectra, but with the total pressure  $P_{tot} = P_{tot}^{meas} + \Delta P$ , where  $\Delta P$  is the error in the measured total pressure. The corresponding uncertainty of the line-shape parameters was then determined as the difference between the parameters obtained using  $(P_{tot}^{meas} + \Delta P)$  and those obtained using  $P_{tot}^{meas}$ . A similar procedure was performed to determine the uncertainty due to the uncertainty of the measured temperature. To account for errors due to the instrumental line-shape function, we performed our fits with two instrument line-shape functions, both determined using LINEFIT, but by applying LINEFIT to some chosen microwindows which contain intense and isolated lines, as well as to the entire R branch in the pure  $\text{CO}_2$  spectrum. In addition, the obtained line-

shape parameters were considered as obtained at the average temperature. The uncertainty due to the difference between the average temperature and the temperature measured for each spectrum was also considered, using the temperature dependence exponent of He-broadening coefficients provided in the HITRAN database [6]. The total uncertainty for each retrieved parameter was then computed as the sum of each individual uncertainty and reported in Table 2 of this paper, together with the parameter values.

## 4. Results and discussions

### 4.1 Broadening coefficient

Figure 3 displays the obtained He-broadening coefficients,  $\gamma_{\text{He}}$ , in the  $\nu_3$  band of  $^{12}\text{CO}_2$ . Literature data (see Fig. 1) are also plotted for comparison. As can be observed in the figure, our results are in very good agreement with the values obtained by Ref. [12] for *R*-branch lines of the same band. The average difference is  $0.9 (\pm 1.3) \%$  (where the number in parentheses corresponds to the standard deviation of the average). In the *P* branch, our values are in excellent agreement with those measured by Ref. [10] for the  $3\nu_3$  band with an average difference of  $1.3 (\pm 1.4) \%$ . However, in the *R* branch, the values from Ref. [10] are significantly larger than our results, as well as data from Ref. [12]. Our results show that the values in the *P* and *R* branches are nearly symmetric in  $m$ , as generally observed for parallel bands of  $\text{CO}_2$  (see Ref. [20] and references therein). We therefore cannot explain the discrepancy in the *P* and *R* branches values reported by Ref. [10]. Additionally, good agreement is found between our data and the theoretically calculated values of Ref. [13], as well as the experimentally determined values of Ref. [9]. The latter were obtained by fitting the measured spectra with a convolution of a Galatry function and a sum of Lorentzians [9], which explains why these values are larger than the others, obtained using the Voigt profile. Finally, we observe a substantial difference between these data (including our results) and the measurements of Ref. [7]. This difference increases with the rotational quantum number: for  $|m| = 8$ , and  $|m| = 38$ , the difference between data from Ref. [7] and our results are about 1% and 5%, respectively. Since the data in HITRAN were fitted to the measured values of Ref. [7], they also differ significantly (smaller) from our values.

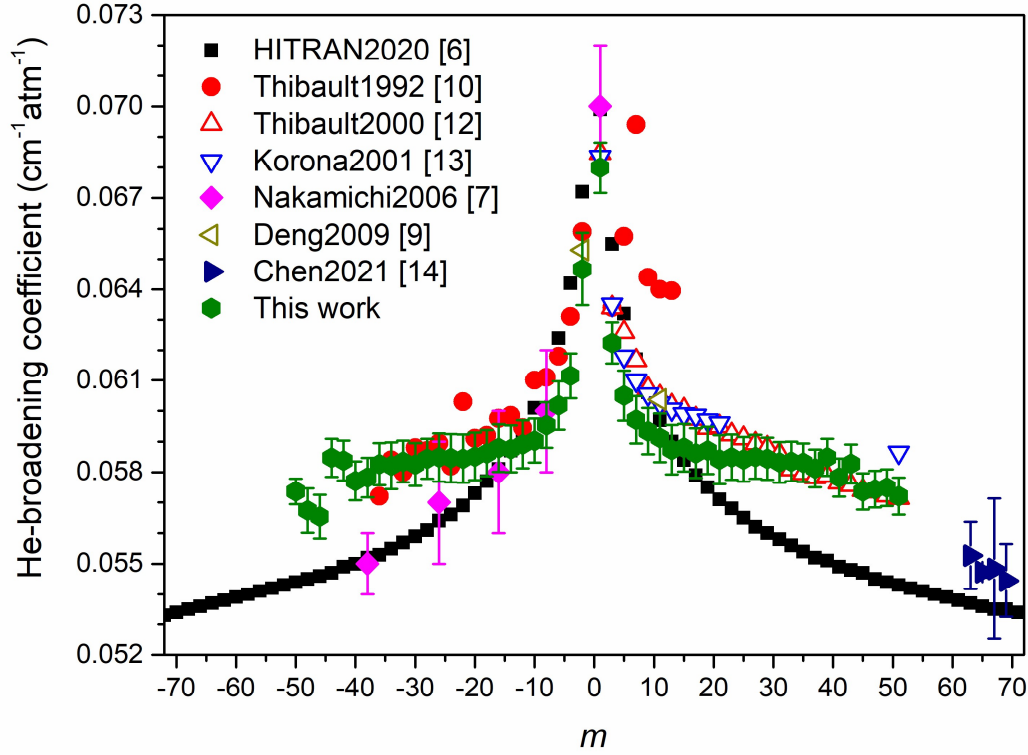


Figure 3: He-broadening coefficients for  $^{12}\text{CO}_2$   $v_3$  lines obtained in this work at 294 K and comparison with measured data from Ref. [10] for the  $3v_3$  band, Ref. [12] for the  $v_3$  band, Ref. [7] for the  $3v_1+v_3$  band, and from Ref. [9] for the  $v_3$  band but of  $^{13}\text{CO}_2$ . Experimental results from Ref. [14] for some high  $J$  lines in the  $v_3$  band and theoretical results from Ref. [13] for the same band are also reported, along with data provided in the 2020 edition of the HITRAN database [6].

We therefore recommend to update the He-broadening coefficients for  $\text{CO}_2$  lines for use in spectroscopic databases and applications. Since there is a very good agreement between our values and those of Ref. [12] (see Fig. 3) in which  $\gamma_{\text{He}}$  was measured for temperatures up to 750 K, we used the high-temperature data from [12] to extrapolate room temperature values of  $\gamma_{\text{He}}$  for high  $J$  lines, from  $J = 50$  to  $J = 86$ . A temperature dependence exponent of 0.5 was adopted for these high  $J$  lines. As explained in Ref. [12], at high  $J$ , collisions are most sensitive to the repulsive part of the intermolecular potential, so the variation of  $\gamma_{\text{He}}$  with temperature should approach the gas kinetic theory limit behavior (i.e. a temperature exponent of 0.5). The obtained results are displayed in Fig. 4. We can observe that for lines with  $40 < J < 50$ , a very good agreement is observed between the values of  $\gamma_{\text{He}}$  measured in this work and those measured at room temperature in Ref. [12], and the extrapolated values from high-temperature measurements of Ref. [12]. The extrapolated values of  $\gamma_{\text{He}}$  for high  $J$  lines can thus be used together with our data, to build a comprehensive database for the He-broadening coefficient of  $\text{CO}_2$  lines.

Similar to the approach used in Ref. [5], we applied a Padé approximant to fit to these values, i.e.:

$$\gamma_{\text{He}}(|m|) = \frac{a_0 + a_1|m| + a_2|m|^2 + a_3|m|^3}{1 + b_1|m| + b_2|m|^2 + b_3|m|^3 + b_4|m|^4}$$



The results of the fit are shown in Fig. 4, together with the current values of HITRAN, while the values of the coefficients  $a_0, a_1, a_2, a_3$  and  $b_1, b_2, b_3$  and  $b_4$  are given in Table 3.

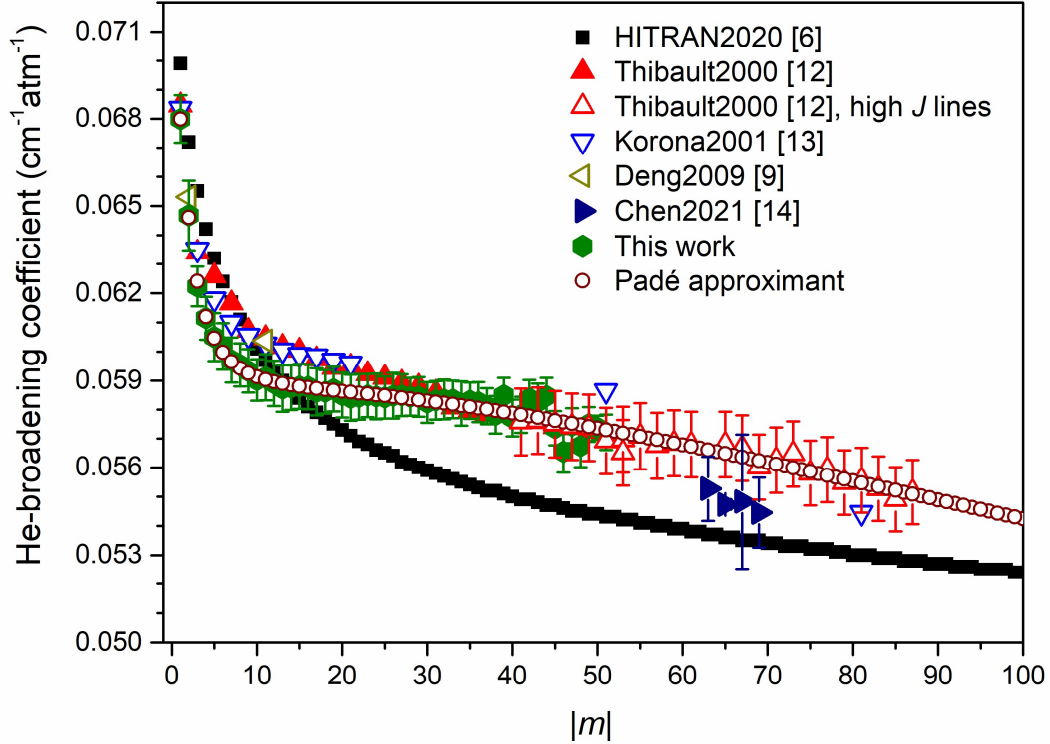


Figure 4: Room temperature He-broadening coefficients as function of  $|m|$ . The Padé approximant was fitted to values obtained in this work for  $|m|$  up to 51 and to values extrapolated from high-temperature data measured by Ref. [12] for higher  $|m|$ . The error bar for the latter corresponds to an uncertainty of 2%. Values from Ref. [12] for  $|m| < 51$  and those of Refs. [9,13,14] were not used in the fit but are plotted for comparison.

Table 3: The Padé approximant coefficients for He-broadening of  $\text{CO}_2$  lines

Parameter	Value	Parameter	Value
$a_0$	-0.91390	$b_1$	-12.45413
$a_1$	1.18311	$b_2$	87.44142
$a_2$	4.91602	$b_3$	3.23526
$a_3$	0.20165	$b_4$	0.00518

#### 4.2 Pressure-shift coefficient

The measured pressure-shift coefficients,  $\delta_{\text{He}}$ , are plotted in Fig. 5a and compared with the measured value of Ref. [9] for the  $R(11)$  line of the  $^{13}\text{CO}_2$   $\nu_3$  band and with those from Ref. [10] for the  $3\nu_3$  band. An excellent agreement is observed between the present study and the result of Ref. [9], while the absolute magnitude of our pressure shifts is well smaller than those reported in Ref. [10]. This discrepancy can be attributed to the well-known strong vibrational dependence of the pressure shift. Additionally, we can observe that the rotational dependence of  $\delta_{\text{He}}$  is relatively weak, in contrast to the cases of air- and self-pressure shifts [21]. This

behavior can be explained by the small well depth of the intermolecular potential for CO<sub>2</sub>-He interactions. An average value of  $-0.52 \times 10^{-3} \text{ cm}^{-1}/\text{atm}$  can be used for all lines in the  $\nu_3$  band. Following Ref. [21], we can assume that the rotational contribution to the He-pressure shift is negligible, and this value arises from the vibrational contribution only. Therefore, the He-pressure shift in the  $3\nu_3$  band should be three times stronger than that in the  $\nu_3$  band, leading to a value of about  $-1.5 \times 10^{-3} \text{ cm}^{-1}/\text{atm}$ , which is in rather good agreement with the values measured by Ref. [10] (see Fig. 5a). It should be noted that our pressure-shift coefficients were obtained by fitting the measured spectra accounting for line-mixing effects using the first-order approximation [22]. When a simple Voigt profile is used (neglecting line-mixing effects), a much larger and unphysical rotational dependence of the retrieved pressure shift coefficients is observed, as demonstrated in Fig. 5b. This behavior is due to the influence of line-mixing effects, which can shift the peak absorption. This is illustrated in the example shown in Fig. 6, which compares the fit residuals obtained with line mixing accounted for and without line mixing. As can be observed, while accounting for line mixing leads to only a slight overall improvement in the fit residuals, it provides a better model of the measured line shape, particularly its asymmetry. As the considered He-pressure shifts are very small, inaccurate modeling of this asymmetry can lead to erroneous retrieved pressure-shift coefficients.

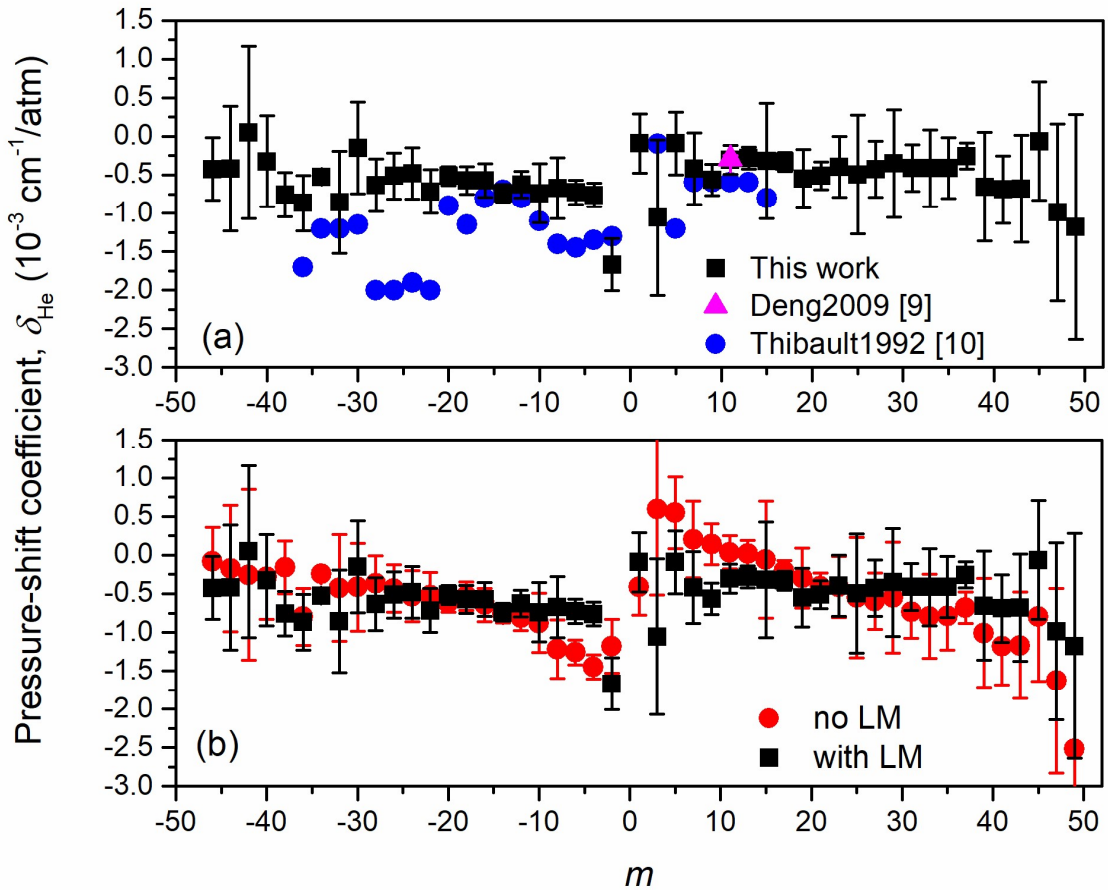


Figure 5: (a) The He-pressure-shift coefficients measured in this work by fitting the experimental spectra using the Voigt profile combined with the first-order line-mixing approximation. These values are compared with the one from Ref. [9] for the  $R(11)$  line of the  $^{13}\text{CO}_2$   $\nu_3$  band and with those from Ref.

[10] for the  $3\nu_3$  band. In panel (b) is the comparison between the pressure shift coefficients obtained from fits that include line-mixing effect and those obtained without accounting for line-mixing.

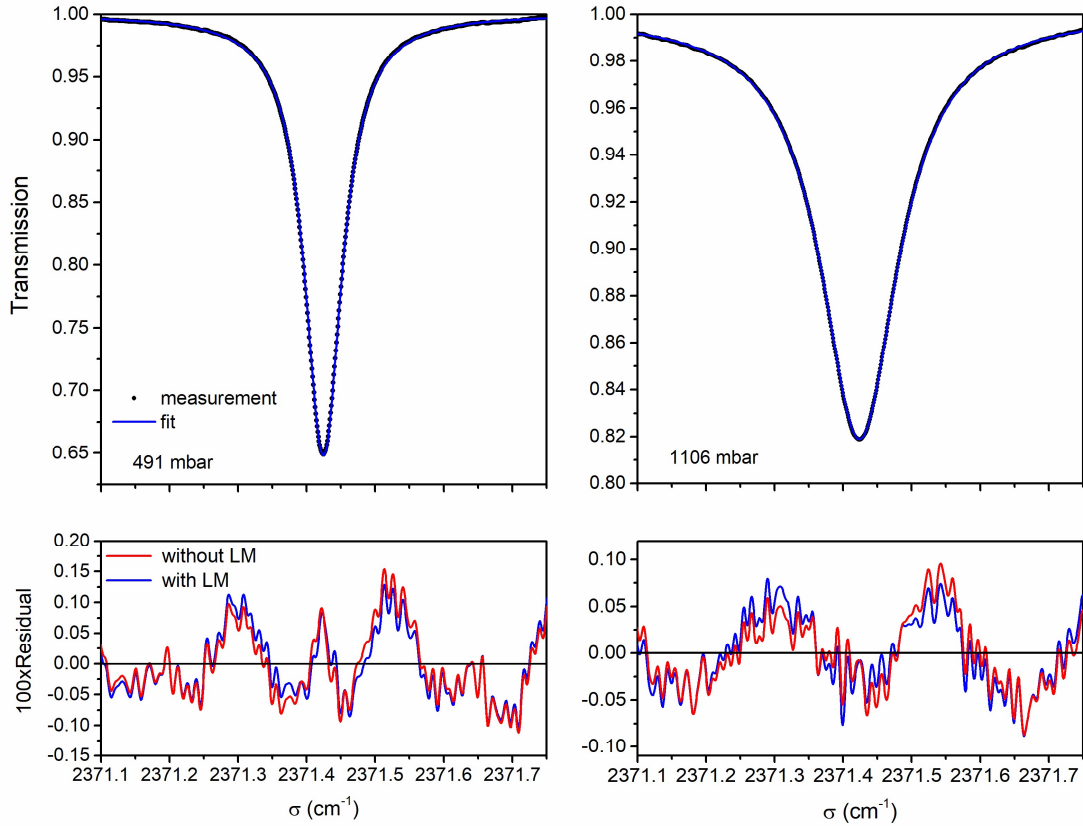


Figure 6: Measured and fitted transmissions (top panel) of the R(33) line, along with the corresponding fit residuals (bottom panel), obtained with line mixing accounted for (blue) and without line mixing (red).

#### 4.3 First-order line-mixing coefficient

Line-mixing effects in the infrared spectrum of CO<sub>2</sub> broadened by He have been investigated in various studies (e.g. [23,24] and references therein), all focused on high-pressure conditions, up to 1000 bar. The observed line-mixing effects were modeled with the Energy Corrected Sudden (ECS) approximation (see Ref. [25] and references therein), which successfully represented the measured spectral shapes for different bands across wide pressure ranges [23,24]. In this study, we used this ECS model with parameters provided in Ref. [24] to compute the relaxation matrix elements for CO<sub>2</sub>-He, following a methodology similar to the one for air- and self-broadened CO<sub>2</sub> matrices in Refs. [26,28]. From this relaxation matrix, we derived the corresponding first-order line-mixing coefficients,  $\xi_{He}$ , for He-broadened CO<sub>2</sub>. The obtained results are used to compare with the coefficients retrieved from our measured spectra, as shown in Fig. 7. As it can be observed, despite being determined from spectra measured at relatively low pressures where line-mixing effects are weak, the values of  $\xi_{He}$  obtained from spectra fits are in rather good agreement with those deduced from the ECS model. This confirms the presence of line-mixing effect for CO<sub>2</sub>-He under the considered pressures and temperature. The measured values of  $\xi_{He}$ , along with their uncertainties, are reported in Table 3, together with the other line-shape parameters.

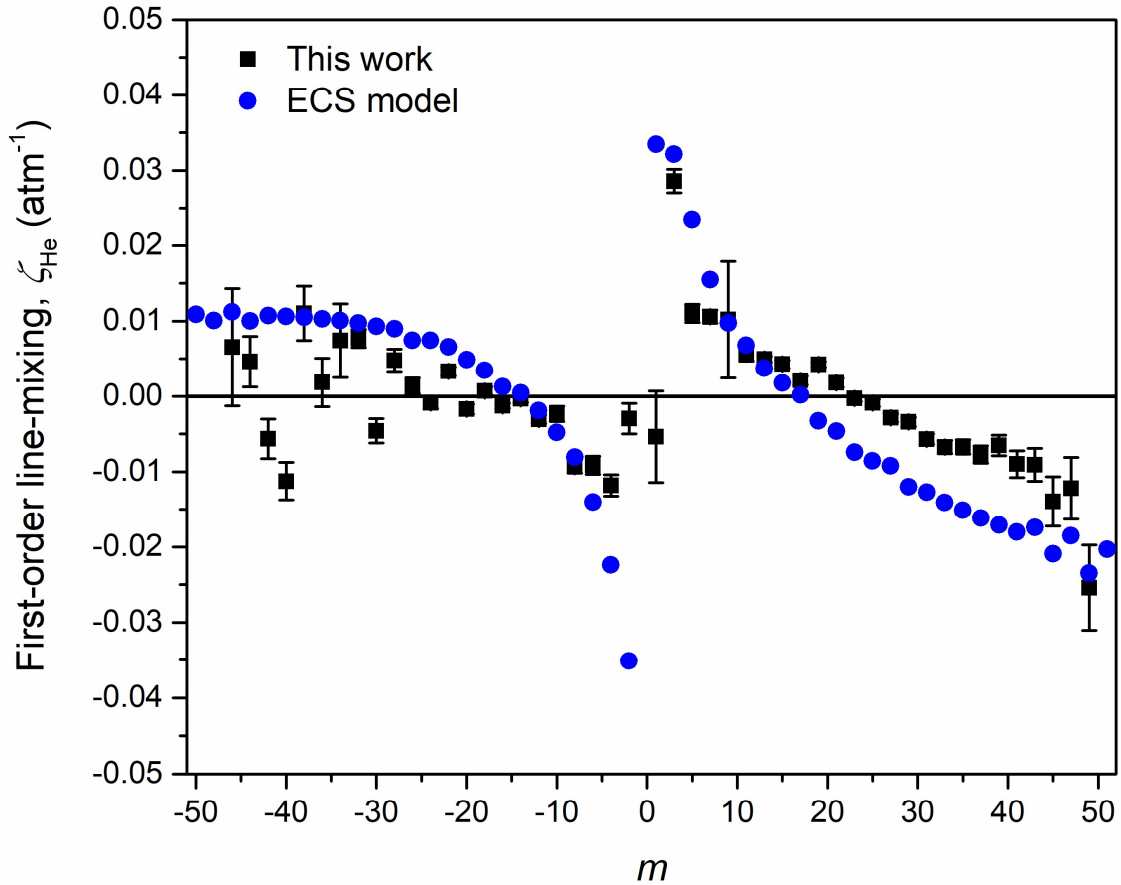


Figure 7: The measured first-order line-mixing coefficients and comparison with those deduced from the ECS model (see text).

## 5. Conclusion

Spectral line-shape parameters were measured for 51 lines of  $^{12}\text{CO}_2$  broadened by He in the  $\nu_3$  band, ranging from the  $P(50)$  to the  $R(51)$  lines at room temperature from transmission spectra recorded with a Fourier transform spectrometer. The measured He-broadening coefficients show excellent agreement with various literature values. Using these broadening coefficients and data for higher  $J$  lines, extrapolated from available high-temperature measurements, we proposed an improved dataset for He-broadening coefficients of  $\text{CO}_2$  lines, suitable for spectroscopic databases and applications. For the first time, He-pressure shift coefficients for were measured the  $\nu_3$  band. The results revealed a very weak rotational dependence of the pressure shift, in contrast to the pronounced dependence observed for self- and air-pressure shifts. Furthermore, we demonstrated that line-mixing effects in the spectra of  $\text{CO}_2$ -He must be considered, even at relatively low pressure, to accurately determine the pressure shifts. The collision-induced line-mixing effect was modeled using the first-order line-mixing approximation. The derived line-mixing coefficients were found to agree well with those calculated using the well-known Energy Corrected Sudden approximation. While this work represents an extensive experimental study of line-shape parameters for  $\text{CO}_2$  in He at room temperature, further experimental and theoretical investigations over a broader range of pressures and temperatures are necessary to support studies of exoplanet atmospheres.

Table 2: The measured room temperature He-broadening coefficient ( $\text{cm}^{-1} \text{atm}^{-1}$ ), pressure shifts ( $10^{-3} \text{cm}^{-1} \text{atm}^{-1}$ ), and first-order line-mixing parameter ( $\text{atm}^{-1}$ ) for  $\text{CO}_2$  lines in the  $\nu_3$  band. *Unc* is the corresponding total uncertainty, in units of the last quoted digit.

<i>Line</i>	$\gamma_{\text{He}}$	<i>unc</i>	$\delta_{\text{He}}$	<i>unc</i>	$\zeta_{\text{He}}$	<i>Unc</i>
P(50)	0.05737	42				
P(48)	0.05674	73				
P(46)	0.05654	71	-0.425	407	0.0065	78
P(44)	0.05847	63	-0.419	809	0.0046	34
P(42)	0.05838	65	0.049	1120	-0.0056	26
P(40)	0.05771	64	-0.326	593	-0.0112	25
P(38)	0.05782	64	-0.757	289	0.0110	36
P(36)	0.05826	69	-0.869	359	0.0019	33
P(34)	0.05821	77	-0.524	72	0.0074	49
P(32)	0.05835	69	-0.859	667	0.0077	12
P(30)	0.05825	70	-0.153	596	-0.0046	16
P(28)	0.05844	65	-0.638	341	0.0048	15
P(26)	0.05848	79	-0.514	298	0.0014	11
P(24)	0.05846	79	-0.483	334	-0.0009	8
P(22)	0.05844	79	-0.718	285	0.0033	6
P(20)	0.05851	78	-0.514	125	-0.0017	7
P(18)	0.05862	76	-0.573	181	0.0007	5
P(16)	0.05879	78	-0.570	220	-0.0013	4
P(14)	0.05876	77	-0.739	118	-0.0004	5
P(12)	0.05891	79	-0.629	174	-0.0031	6
P(10)	0.05903	72	-0.739	384	-0.0024	11
P(8)	0.05954	74	-0.673	398	-0.0093	9
P(6)	0.06018	79	-0.726	156	-0.0092	12
P(4)	0.06115	74	-0.763	156	-0.0118	15
P(2)	0.06467	119	-1.670	336	-0.0030	20
R(1)	0.06799	83	-0.092	385	-0.0054	61
R(3)	0.06224	68	-1.060	1010	0.0286	16
R(5)	0.0605	82	-0.092	405	0.0110	12
R(7)	0.05971	77	-0.417	464	0.0106	9
R(9)	0.05934	76	-0.564	206	0.0102	77
R(11)	0.05912	80	-0.302	188	0.0056	9
R(13)	0.05873	81	-0.281	141	0.0049	4
R(15)	0.0588	78	-0.319	753	0.0043	5
R(17)	0.05862	82	-0.330	123	0.0021	6
R(19)	0.05871	77	-0.553	382	0.0043	4
R(21)	0.05841	80	-0.514	182	0.0018	6
R(23)	0.05849	75	-0.394	396	-0.0003	5
R(25)	0.05842	73	-0.497	774	-0.0009	5
R(27)	0.0585	72	-0.429	366	-0.0029	6
R(29)	0.05844	69	-0.351	699	-0.0034	6
R(31)	0.05832	67	-0.411	306	-0.0057	7
R(33)	0.05835	65	-0.415	502	-0.0067	9
R(35)	0.05831	63	-0.414	397	-0.0067	10
R(37)	0.05812	62	-0.256	170	-0.0077	12
R(39)	0.05849	61	-0.654	710	-0.0065	14
R(41)	0.05782	62	-0.691	437	-0.0090	18
R(43)	0.05827	64	-0.679	695	-0.0091	22
R(45)	0.05736	60	-0.062	766	-0.0140	33

R(47)	0.05744	61	-0.986	1150	-0.0122	41
R(49)	0.05749	60	-1.180	1460	-0.0254	56
R(51)	0.05721	61				

## References

- [1] Atreya SK, Wong MH, Owen TC, Mahaffy PR, Niemann HB, de Pater I, Drossart P, Encrenaz T. A comparison of the atmospheres of Jupiter and Saturn: deep atmospheric composition, cloud structure, vertical mixing, and origin. *Planet Space Sci* 1999;47:1243-62.
- [2] Lara LM, Rodrigo R, Moreno R, Lampón M. Analysis of the origin of water, carbon monoxide, and carbon dioxide in the Uranus atmosphere. *A&A* 2019;621:A129.
- [3] Fortney JJ, Robinson TD, Domagal-Goldman S, Genio ADD, Gordon IE, Gharib-Nezhad E, Lewis N, Sousa-Silva C, Airapetian V, Drouin B, Hargreaves RJ, et al. The Need for Laboratory Measurements and Ab Initio Studies to Aid Understanding of Exoplanetary Atmospheres. *Astro2020 Science White Paper*. <https://escholarship.org/uc/item/3db4r31q>
- [4] Chubb KL, Robert S, Sousa-Silva C, Yurchenko SN, Allard NF, Boudon V, Buldyreva J, Bultel B, Coustenis A, Foltynowicz A, Gordon IE, et al. Data availability and requirements relevant for the Ariel space mission and other exoplanet atmosphere applications. *RAS Techniques and Instruments* 2024;3:636-90, <https://doi.org/10.1093/rasti/rzac039>
- [5] Tan Y, Skinner FM, Samuels S, Hargreaves RJ, Hashemi R, Gordon IE. H<sub>2</sub>, He, and CO<sub>2</sub> pressure-induced parameters for the HITRAN database. II. Line mixes of CO<sub>2</sub>, N<sub>2</sub>O, CO, SO<sub>2</sub>, OH, OCS, H<sub>2</sub>CO, HCN, PH<sub>3</sub>, H<sub>2</sub>S, and GeH<sub>4</sub>. *The Astrophysical Journal Supplement Series*, 2022;262:40.
- [6] Gordon IE, Rothman LS, Hargreaves RJ, Hashemi R, Karlovets EV, Skinner FM, Conway EK, Hill C, Kochanov RV, Tan Y, Wcisło P, Finenko AA, Nelson K, Bernath PF, Birk M, Boudon V, Campargue A, Chance KV, ..., Yurchenko SN. The HITRAN2020 molecular spectroscopic database. *J Quant Spectrosc Rad Transf* 2022;277:107949. <https://doi.org/10.1016/j.jqsrt.2021.107949>
- [7] Nakamichi S, Kawaguchi Y, Fukuda H, Enami S, Hashimoto S, Kawasaki M, Umekawa T, Morino I, Sutoc H, Inoue G. Buffer-gas pressure broadening for the (3001)<sub>III</sub> ← (0000) band of CO<sub>2</sub> measured with continuous-wave cavity ring-down spectroscopy. *Phys Chem Chem Phys* 2005;8:364-68.
- [8] Brimacombe RK, Reid RK. Accurate measurements of pressure-broadened linewidths in a transversely excited CO<sub>2</sub> discharge. *IEEE Journal of Quantum Electronics* 1983;19:1668-73.
- [9] Deng W, Mondelain D, Thibault F, Camy-Peyret C, Mantz AW. Experimental He-pressure broadening for the R(10) and P(2) lines in the ν<sub>3</sub> band of <sup>13</sup>CO<sub>2</sub>, and experimental pressure shifts for R(10) measured at several temperatures between 300 K and 100 K. *J Mol Spectrosc* 2009; 256:102-8.
- [10] Thibault F, Boissoles J, Le Doucen R, Bouanich JP, Arcas P, Boulet C. Pressure induced shifts of CO<sub>2</sub> lines: Measurements in the 003–000 band and theoretical analysis. *J Chem Phys* 1992;96:4945-53. <https://doi.org/10.1063/1.462737>.
- [11] Ozanne L, Bouanich JP, Rodrigues R, Hartmann JM, Blanquet JM, Walrands JM. Diode-laser measurements of He- and N<sub>2</sub>- broadening coefficients and line-mixing effects in the Q-branch of the ν<sub>1</sub>-ν<sub>2</sub> band of CO<sub>2</sub>. *J Quant Spectrosc Radiat Transfer* 1998;59:337-44.

- [12] Thibault F, Calil B, Boissoles J, Launay JM. Experimental and theoretical CO<sub>2</sub>-He pressure broadening cross sections. *Phys Chem Chem Phys* 2000;2:5404-10.
- [13] Korona T, Moszynski R, Thibault F, Launay JM, Bussery-Honvault B, Boissoles J, Wormer PES. Spectroscopic, collisional, and thermodynamic properties of the He-CO<sub>2</sub> complex from an ab initio potential: Theoretical predictions and confrontation with the experimental data. *J Chem Phys* 2001;115:3074-84. <https://doi.org/10.1063/1.1385524>
- [14] Chen D, Shi L, Xu P, Wang R, Zhang C. Buffer-gas pressure broadening at high J values in the  $\nu_3$  band of CO<sub>2</sub> measured with tunable diode laser absorption spectroscopy. *J Mol Spectrosc*, 2021;377:111429.
- [15] Mertz L. *Transformations in Optics*. John Wiley and Sons, New York, 1965.
- [16] Hase F, Blumenstock T, Paton-Walsh C. Analysis of the instrumental line shape of high-resolution Fourier transform IR spectrometers with gas cell measurements and new retrieval software. *Appl Opt* 1999;38:3417-22.
- [17] Hase F. Improved instrumental line shape monitoring for the ground-based, high-resolution FTIR spectrometers of the Network for the Detection of Atmospheric Composition Change. *AMT* 2012;5:603-10.
- [18] Ngo NH, Lisak D, Tran H, Hartmann JM. An isolated line-shape model to go beyond the Voigt profile in spectroscopic databases and radiative transfer codes. *J Quant Spectrosc Radiat Transf* 2013, 129, 89-100.
- [19] Tennyson J, Bernath P, Campargue A, Csaszar AG, Daumont L, Gamache RR, Hodges JT, Lisak D, Naumenko OV, Rothman LS, Tran H, Zobov NF, Buldyreva J, Boone C, De Vizia MD, Gianfrani L, Hartmann JM, McPheat R, Weidmann D, Murray J, Ngo NH, Polyansky OL. Recommended isolated line profile for representing high-resolution spectroscopic transitions. *P Appl Chem* 2014;86:1931-43.
- [20] Hashemi R, Gordon IS, Tran H, Kochanov RV, Karlovets EV, Tan Y, Lamouroux J, Ngo NH, Rothman LS. Revising the line-shape parameters for air- and self-broadened CO<sub>2</sub> lines toward a sub-percent accuracy level. *J Quant Spectrosc Rad Transf* 2020;256:107283.
- [21] Hartmann JM. A simple empirical model for the collisional spectral shift of air-broadened CO<sub>2</sub> lines. *J Quant Spectrosc Rad Transf* 2009;110:2019-26.
- [22] Rosenkranz PW. Shape of the 5 mm oxygene band in the atmosphere. *IEEE Trans. Antennas Propag* 1975; AP-23:498-506.
- [23] Ozanne L, Nguyen-Van-Thanh, Brodbeck C, Bouanich JP, Hartmann JM, Boulet C. Line mixing and nonlinear density effects in the  $\nu_3$  and  $3\nu_3$  infrared bands of CO<sub>2</sub> perturbed by He up to 1000 bar. *J Chem Phys* 1995;102:7306-16.
- [24] Rodrigues R, Khalil B, Le Doucen R, Bonamy L, Hartmann JM. Temperature, pressure, and perturber dependencies of line-mixing effects in CO<sub>2</sub> infrared spectra. I.  $\Sigma$ - $\Pi$  Q branches. *J Chem Phys* 1997;107:4118-32
- [25] Hartmann JM, Boulet C, Robert D. *Collisional effects on molecular spectra. Laboratory experiments and model, consequences for applications*. Elsevier, Amsterdam 2008.
- [26] Lamouroux J, Régalia L, Thomas X, Vander Auwera J, Gamache RR, Hartmann JM. CO<sub>2</sub> line-mixing database and software update and its tests in the 2.1  $\mu\text{m}$  and 4.3  $\mu\text{m}$  regions. *J Quant Spectrosc Rad Transf* 2015;151:88-96.

- [27] Tran H, Boulet C, Stefania S, Snels M, Piccioni G. Measurements and modeling of high-pressure pure CO<sub>2</sub> spectra from 750 to 8500 cm<sup>-1</sup>. I-central and wing regions of the allowed vibrational bands. *J Quant Spectrosc Radiat Transfer* 2011;112:925-36.
- [28] Cole RK, Tran RK, Hoghooghi RK, Rieker GB. Temperature-dependent CO<sub>2</sub> line mixing models using dual frequency comb absorption and phase spectroscopy up to 25 bar and 1000 K. *J Quant Spectrosc Radiat Transf* 2023;297:108488.